J Geod (2009) 83:13–29
DOI 10.1007/s00190-008-0225-x

ORIGINAL ARTICLE

Optimal multi-step collocation: application to the space-wise approach for GOCE data analysis

Mirko Reguzzoni · Nikolaos Tselfes

Received: 18 June 2007 / Accepted: 17 March 2008 / Published online: 15 May 2008

Abstract Collocation is widely used in physical geodesy. Its application requires to solve systems with a dimension equal to the number of observations, causing numerical problems when many observations are available. To overcome this drawback, tailored step-wise techniques are usually applied. An example of these step-wise techniques is the space-wise approach to the GOCE mission data processing. The original idea of this approach was to implement a two-step procedure, which consists of first predicting gridded values at satellite altitude by collocation and then deriving the geopotential spherical harmonic coefficients by numerical integration. The idea was generalized to a multi-step iterative procedure by introducing a time-wise Wiener filter to reduce the highly correlated observation noise. Recent studies have shown how to optimize the original two-step procedure, while the theoretical optimization of the full multi-step procedure is investigated in this work. An iterative operator is derived so that the final estimated spherical harmonic coefficients are optimal with respect to the Wiener–Kolmogorov principle, as if they were estimated by a direct collocation. The logical scheme used to derive this optimal operator can be applied not only in the case of the space-wise approach but, in general, for any case of step-wise collocation. Several numerical tests based on simulated realistic GOCE data are performed. The results show that adding a pre-processing time-wise filter to the two-step procedure of data gridding and spherical harmonic analysis is useful, in the sense that the accuracy of the estimated geo-potential coefficients is improved. This happens because, in its practical implementation, the gridding is made by collocation over local patches of data, while the observation noise has a time-correlation so long that it cannot be treated inside the patch size. Therefore, the multi-step operator, which is in theory equivalent to the two-step operator and to the direct collocation, is in practice superior thanks to the time-wise filter that reduces the noise correlation before the gridding. The criteria for the choice of this filter are investigated numerically.

Keywords Earth's gravity field · GOCE mission · Space-wise approach · Collocation · Wiener filter

M. Reguzzoni
Geophysics of the Lithosphere Department,
Italian National Institute of Oceanography and Applied Geophysics, c/o Politecnico di Milano, Polo regionale di Como,
Via Valleggio 11, 22100 Como, Italy
e-mail: mirko@geomatica.como.polimi.it

N. Tselfes (✉)
DIIAR, Politecnico di Milano, Polo regionale di Como,
Via Valleggio 11, 22100 Como, Italy
e-mail: nikos@geomatica.como.polimi.it

1 Introduction

GOCE (Gravity field and steady-state Ocean Circulation Explorer) is a satellite mission designed by ESA (European Space Agency) that will be launched in 2008 (ESA 1999; Drinkwater et al. 2007). The main information delivered by GOCE will be measurements of the second order derivatives of the gravitational potential (gravity gradients), obtained from the on-board gradiometer, and tracking data of the satellite orbit from the GPS receiver. The goal of this mission is the determination of a global model of the Earth gravitational field with high accuracy and resolution (2 cm error in terms of geoid undulation at 100 km resolution).

A consortium that comprises European universities and research centres has been formed with the task to organize the data analysis (Rummel et al. 2004). This analysis includes effective pre-processing (Bouman et al. 2007), high-accuracy

satellite positions and velocities estimation (Visser et al. 2007), gravitational field determination in terms of spherical harmonic expansion, and delivery of other output data for scientific applications (Gruber et al. 2007). Three methods are applied for the estimation of the global model, namely the direct approach (Bruinsma et al. 2004), the time-wise approach (Pail et al. 2005) and the space-wise approach (Migliaccio et al. 2004a). Other methods have been proposed outside this consortium, e.g. see Klees et al. (2003).

In the space-wise approach, first the potential values are estimated by the energy conservation method using the derived satellite positions and velocities and the measured non-gravitational accelerations (Jekeli 1999; Visser et al. 2003). Then, these potential values and the measured gravity gradients are used for the computation of spherical grids of potential and second order radial derivatives at satellite altitude. The gridding is based on local patches of data, because global gridding would be computationally impossible due to the several millions of observations. From these gridded data, the coefficients of the global model are estimated by spherical harmonic analysis based on numerical integration (Colombo 1981). Before the gridding, the observations are filtered by a Wiener filter (Papoulis 1984) along the orbit to reduce the heavily coloured noise of the gravity gradients. The procedure is iterated to achieve an optimal combination of time-wise filtering and space-wise collocation and also to take into account the attitude variations of the gradiometer.

Recently, the sufficiency of two-step collocation procedures with respect to the direct solution has been studied in general (Reguzzoni et al. 2006). The specific case of the two-step procedure consisting of gridding and numerical integration for spherical harmonic coefficients estimation has been investigated in Migliaccio et al. (2007b), where it is also discussed how to choose the patch size of the data gridding and which intermediate functionals to predict. The impact of the Wiener filter to the final space-wise approach solution is studied here.

In Sect. 2, the derivation of the Wiener filter is illustrated. It is found that the covariances computed in a time-wise sense do not represent properly the stochastic structure of the signal and consequently the computed filter is not optimal in the sense of minimizing the estimation error variance (Wiener–Kolmogorov principle). This must be taken into account in the subsequent steps. Three questions are treated: 1) how the optimal solution involving the Wiener filter can be obtained, 2) if the use of the filter is really necessary and, if this is the case, 3) how this filter has to be chosen when the target is to achieve the best accuracy of the estimated spherical harmonic coefficients. The first question is answered theoretically in Sect. 3, while the second and third questions are answered by numerical experiments on simulated GOCE data in Sect. 4.

Table 1 Data types and their codes

Data type	Index i, j, k
T	0
$T_{\xi\xi}$	1
$T_{\xi\eta}$	2
$T_{\xi r}$	3
$T_{\eta\eta}$	4
$T_{\eta r}$	5
T_{rr}	6

2 The use of Wiener filter to GOCE data

The observations employed in the space-wise approach are the gravitational potential, denoted as T, and six gravity gradients denoted as $T_{\xi\xi}, T_{\xi\eta}, T_{\xi r}, T_{\eta\eta}, T_{\eta r}$ and T_{rr}. These symbols represent the second order derivatives of the potential along the axes of the Local Orbital Reference Frame (LORF) with ξ pointing almost along-track, η cross-track and r radial. Note that, in a so-defined frame, the axis ξ would be exactly along-track only if the orbit were circular.

The observations are considered as functions of time t and are denoted as $b_i(t)$. The observations consist of the signal $y_i(t)$ and the noise $v_i(t)$:

$$b_i(t) = y_i(t) + v_i(t). \tag{1}$$

The index i discriminates among the different data types, i.e. the potential is labelled with 0 and the gravity gradients with 1 to 6 (see Table 1). When a combination of different data types is used, then the indexes j and k will be introduced.

In order to reduce the noise $v_i(t)$, a time-wise Wiener filter is applied. The derivation of this filter and its relation to the gravitational field is presented in the following.

2.1 The derivation of the Wiener filter

A filtered version of every data type at time t^0 is obtained by applying:

$$\hat{y}_i\left(t^0\right) = \sum_{j\in J} \int_{-\infty}^{+\infty} b_j(t) h^0_{(i)(j)}(t)\,\mathrm{d}t, \tag{2}$$

where $\hat{y}_i\left(t^0\right)$ refers to a single estimate at time t^0 and $h^0_{(i)(j)}(t)$ is the time-wise kernel that depends on the time t^0. The index i refers to the data being filtered and is fixed. The index j refers to the observations that are used to filter the data type i and takes the values of a set J. For example, if the gravity gradients T_{rr} are processed, then i is fixed to 6 and if the same T_{rr} observations plus the observations of T and of $T_{\xi\xi}$ are used to compute the filtered version of T_{rr} then J is $\{0, 1, 6\}$. Note that data are assumed to be continuous in time, though in a real case only a finite, discrete series of

observations is available. This is convenient for the following derivations.

Assuming that signal and noise are random and stationary processes with zero mean and known covariance function, then the variance of the estimation error

$$e_i\left(t^0\right) = y_i\left(t^0\right) - \hat{y}_i\left(t^0\right) \tag{3}$$

is (Sansò and Sideris 1997):

$$\begin{aligned}\sigma_e^2\left[\left\{h^0_{(i)(k)}(t)\right\}\right] &= C_{y(i)y(i)}(0)\\ &+\sum_{j\in J}\sum_{k\in J}\int_{-\infty}^{+\infty}\int_{-\infty}^{+\infty} C_{b(j)b(k)}\left(t-t'\right)h^0_{(i)(k)}(t)h^0_{(i)(j)}(t')\mathrm{d}t\,\mathrm{d}t'\\ &-2\sum_{k\in J}\int_{-\infty}^{+\infty} C_{y(i)b(k)}\left(t-t^0\right)h^0_{(i)(k)}(t)\,\mathrm{d}t.\end{aligned} \tag{4}$$

The functions $C_{y(j)y(k)}(\tau)$ and $C_{b(j)b(k)}(\tau)$, with $\tau = |t-t'|$, $\tau \in R^1$, are the covariance functions (for $j = k$) or the cross-covariance functions (for $j \neq k$) of the signal and of the observations, respectively. The functions $C_{y(j)b(k)}(\tau)$ are the cross-covariance functions between the signal and the observations. If signal and noise are considered uncorrelated, then the function $C_{y(j)b(k)}(\tau)$ is equal to $C_{y(j)y(k)}(\tau)$ and the function $C_{b(j)b(k)}(\tau)$ is equal to the sum of $C_{y(j)y(k)}(\tau)$ plus $C_{v(j)v(k)}(\tau)$. Note that the error variance depends on the kernels $h^0_{(i)(k)}(t)$, $\forall k \in J$.

According to the Wiener–Kolmogorov principle, these kernels are chosen so that the error variance is minimized. In order to minimize an integral expression, the first variation of this expression with respect to each unknown function must be set equal to zero (Bronshtein et al. 2004); therefore, the minimum of Eq. (4) is obtained when, $\forall k \in J$, it holds that:

$$\sum_{j\in J}\int_{-\infty}^{+\infty} C_{b(j)b(k)}\left(t-t'\right)h^0_{(i)(j)}\left(t'\right)\mathrm{d}t' = C_{y(i)b(k)}\left(t-t^0\right). \tag{5}$$

This results in a system of equations with a dimension equal to the number of elements of J. This system can be conveniently solved by Fourier methods (Sansò and Sideris 1997).

We define $S_{b(j)b(k)}(f)$ as the Fourier transform of the corresponding covariance function (for $j = k$) or cross-covariance function (for $j \neq k$) of the observations and $S_{y(i)b(k)}(f)$ as the Fourier transform of the corresponding cross-covariance function between the signal and the observations. We also define $H^0_{(i)(j)}(f)$ as the Fourier transform of the function $h^0_{(i)(j)}(t)$. The Fourier transforms of covariance functions are known as power spectra and are functions of the frequency f (Blackman and Tukey 1958). The Fourier transforms of cross-covariance functions are denoted as power cross-spectra. Throughout the GOCE data treatment, we assume that cross-covariance functions are symmetric, since, after numerical tests, the imaginary part of the corresponding power cross-spectra is found to be negligible. Therefore, all the power spectra and power cross-spectra are real and from now on their imaginary parts will be ignored. The system of Eq. (5) reads in the frequency domain as:

$$\sum_{j\in J} S_{b(j)b(k)}(f)\,H^0_{(i)(j)}(f) = S_{y(i)b(k)}(f)\,e^{\iota 2\pi f t^0}. \tag{6}$$

Note that the time shift for t^0 in Eq. (5) corresponds to a multiplication by the term $e^{\iota 2\pi f t^0}$ in the frequency domain, where ι is the imaginary unit.

Now it is possible to define a function $h_{(i)(j)}(t)$ so that its Fourier transform $H_{(i)(j)}(f)$ has the property:

$$H^0_{(i)(j)}(f) = H_{(i)(j)}(f)\,e^{\iota 2\pi f t^0}. \tag{7}$$

In other words, the optimal kernel is the same for every point in time, with a proper time shift, i.e.:

$$h^0_{(i)(j)}(t) = h_{(i)(j)}\left(t-t^0\right). \tag{8}$$

If Eq. (8) is inserted into Eq. (2) and if t^0 is now considered as a variable instead of a fixed point in time, then the filtering of every data type i for the complete time-series is actually a sum of convolutions. To avoid matrix-vector notation, the following line of thought is used: it is assumed that, frequency by frequency, the matrix composed by the elements $S_{b(j)b(k)}(f)$ for $j,k \in J$ is invertible and the elements of the inverse matrix are denoted as $S_{b(j)b(k)}(f)^{-1}$. Inserting Eq. (7) into Eq. (6) and simplifying the time shift term, it holds that:

$$H_{(i)(j)}(f) = \sum_{k\in J} S_{b(j)b(k)}(f)^{-1}\,S_{y(i)b(k)}(f). \tag{9}$$

This result is the same as in Sideris (1996) and Andritsanos et al. (2001) for the so-called "two-input output system theory method".

The system of Eq. (5) is approximated with the available discrete data of constant and high sampling rate and it becomes a typical collocation system with Toeplitz form covariance matrices. Therefore, the kernels are practically the same for all points and collocation in time is a convolution that can be more conveniently applied in the frequency domain. However, the kernels are different for points at the edges of the time-series; this is due to the fact that the inverse of a Toeplitz matrix is not Toeplitz any more (Schuh 1996). In other words, the spectral Wiener filter is a time-wise collocation, except that it does not adapt to the edges of the available time-series; in addition, there is the cyclical convolution error that can be eliminated by using zero-padding schemes (Jekeli 1998).

If one data type is used (no combinations are made) and no correlation between signal and noise is considered, then Eq. (9) degenerates to the classic definition of the Wiener filter (Papoulis 1984):

$$H_{(i)(i)}(f) = \frac{S_{y(i)y(i)}(f)}{S_{y(i)y(i)}(f) + S_{v(i)v(i)}(f)}. \tag{10}$$

To conclude the Wiener filter analysis, expressions of the error power cross-spectra are given, even though they are not actually used in the space-wise approach implementation. The error power cross-spectrum $S_{e(i)e(l)}(f)$ is defined as the Fourier transform of the cross-covariance function between the estimation error (Eq. 3) of two different data types i and l. Note that if $i = l$ then we have the error power spectrum. It holds that:

$$\begin{aligned} S_{e(i)e(l)}(f) = {} & S_{y(i)y(l)}(f) \\ & - \sum_{j\in J} S_{b(i)y(j)}(f)\, H_{(l)(j)}(f) \\ & - \sum_{j\in J} S_{y(l)b(j)}(f)\, H_{(i)(j)}(f) \\ & + \sum_{j\in J}\sum_{k\in J} H_{(i)(j)}(f)\, S_{b(j)b(k)}(f)\, H_{(l)(k)}(f). \end{aligned} \tag{11}$$

Since the filters used are those according to Eq. (9), then Eq. (11) reads simply:

$$\begin{aligned} S_{e(i)e(l)}(f) = {} & S_{y(i)y(l)}(f) \\ & - \sum_{j\in J}\sum_{k\in J} S_{y(i)b(j)}(f)\, S_{b(j)b(k)}(f)^{-1}\, S_{b(k)y(l)}(f). \end{aligned} \tag{12}$$

2.2 Limitation of the Wiener filter along the orbit

Equations of Sect. 2.1 hold for any signal $y_i(t)$ for $t \in R^1$. However, this is not the case for the gravity field, which is a space-related and not time-related signal. There is some similarity between time distances and spherical distances of the satellite positions for short arcs; in this sense, the time-wise gravity signal covariance function is appropriate (Albertella et al. 2004). However, after half an orbit, the satellite spherical distance with respect to a certain reference point decreases, while the time distance does not, so this similarity is lost. Also, the orbit may vary in such a way that the satellite does not return close to the reference point at regular time intervals. Therefore, the time-wise signal covariance function does not describe the real signal correlation. In fact, an empirical signal covariance function computed from the data in a time-wise fashion is too smooth after a certain time distance and local maxima of the covariance function (caused by the satellite returning to the same areas) are missing.

Moreover, the covariance matrix derived from the time-wise signal covariance function is Toeplitz in the case of constant sampling rate. However, since the signal cannot be considered stationary in time after half an orbit, a Toeplitz matrix is only a limited approximation of the true covariance matrix. For example, if the satellite passes 100 times over the same area, then the 99 local covariance maxima of the satellite returning are lost, and this is a poor (at the level of 1%) approximation of the true covariance matrix.

On the basis of this consideration, signal and noise power spectra are smoothed by a convolution with a window function (Blackman and Tukey 1958) that forces the corresponding covariance functions to zero after a quarter of an orbit. In this way, the time-wise filtering is only applied on points of the same arc and, in particular, over an interval not exceeding half an orbit. The corresponding signal covariance matrix is now band-diagonal, i.e. covariance blocks away from the diagonal are ignored (as if the observations did not exist) instead of being poorly approximated. Also the noise covariance matrix is made band-diagonal, i.e. the noise correlation of distant points is not considered. The resulting filter is thus localized but without splitting the data sets into parts.

In the case of GOCE observations, the noise is considered as a time-correlated phenomenon (ESA 1999; Pail et al. 2005; Reguzzoni 2003) and, therefore, a time-wise noise covariance function is appropriate. Nevertheless, due to the time-wise approximation of the signal covariance functions, the applied Wiener filter is not optimal and this must be taken into account in the sequel. Also the error propagation is not proper because all the signal correlations between distant points in time cannot be propagated. This problem can be overcome as explained in Sect. 3.

3 Optimization of the multi-step collocation procedure

3.1 Two-step optimal solution

First, an important result about step-wise procedures is briefly recalled (Reguzzoni et al. 2006). According to the Wiener–Kolmogorov principle, the optimal solution would be to estimate the spherical harmonic coefficients of the gravitational potential directly with a global collocation (Tscherning 2001):

$$\hat{x} = C_{xb} C_{bb}^{-1} b, \tag{13}$$

where b are the observations, $\hat{x}$ are the coefficient estimates, C_{bb} is the covariance matrix of the observations and C_{xb} is the cross-covariance matrix between the coefficients and the observations.

Assume that intermediate grid values z are first estimated:

$$\hat{z} = C_{zb} C_{bb}^{-1} b, \tag{14}$$

where now C_{zb} is the cross-covariance matrix between the grid values and the observations. If the functionals predicted

on the grid are considered to be a linear combination of the coefficients that is realized by the matrix A of full column rank (in a band-limited approximation), then the relation

$$z = Ax \tag{15}$$

can be inverted:

$$x = \left(A^T A\right)^{-1} A^T z = Bz. \tag{16}$$

The use of Eq. (16) to estimate the coefficients x gives rise to the same solution of the direct collocation, i.e. no information is lost in this two-step procedure:

$$\hat{\hat{x}} = B\hat{\hat{z}} = BC_{zb}C_{bb}^{-1}b = C_{xb}C_{bb}^{-1}b = \hat{x}. \tag{17}$$

In the case of GOCE, there are so many observations that a direct collocation to estimate the spherical harmonic coefficients is not possible and therefore an intermediate grid is computed. For the same reason, the gridding cannot be made by a unique collocation system, but it is realized by means of many localized systems, i.e. using local patches of data. Therefore, information is lost because of the patch-wise collocation (Migliaccio et al. 2007b). Moreover, the signal is not band-limited in reality, though the gradiometer signal at satellite altitude (about 250 km) and above a certain spherical harmonic degree (e.g. 360) is not significant with respect to the noise level.

The linear operator B, which is used to transform gridded data to spherical harmonic coefficients (Eq. 16), is implemented by numerical integration (Colombo 1981) and is not exact because of discretization errors. These errors are not significant when high resolution grids are used (Migliaccio et al. 2007b).

However, how is the optimal estimation found when another filter (in this case the Wiener filter along the orbit) is first applied to the data? Is there information lost because of this filter? These questions are answered in the next section.

3.2 Iterative multi-step optimal solution

We define the matrix W as the Wiener filter for all the used data types in the time domain, i.e. W is a block matrix, where each block is Toeplitz, representing the convolution operator by the kernels $h_{(i)(j)}(t)$. Therefore all the data filtered together are:

$$\hat{y} = Wb. \tag{18}$$

The optimal solution for the grid is:

$$\hat{z} = C_{zy}W^T \left(WC_{yy}W^T + WC_{vv}W^T\right)^{-1} \hat{y}, \tag{19}$$

under the assumption that:

$$C_{bb} = C_{yy} + C_{vv}. \tag{20}$$

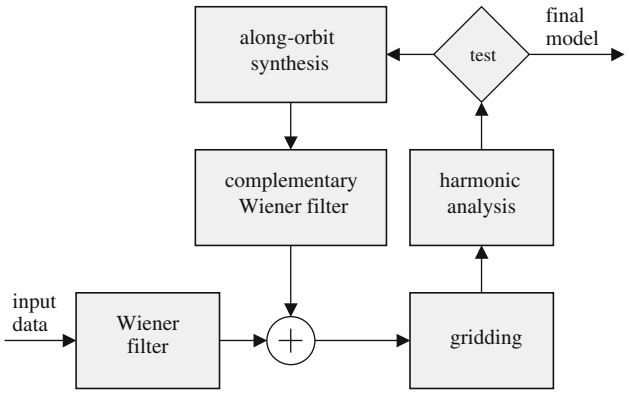

Fig. 1 Basic flow-chart of the space-wise solution

It can be verified that if Eq. (18) is substituted in Eq. (19), then the classic collocation formula is obtained (Eq. 14), under the hypothesis that W is invertible. In general, it is possible that the original data are projected onto a smaller space, i.e. W is not invertible (Basilevsky 1983). In such a case, some frequencies vanish and information is lost; in other words the filtered data would be linear combinations of fewer Fourier base functions than the original data.

In order to obtain the optimal estimation on the grid, Eq. (19) should be applied. However, this is not possible because, as stated before, a global collocation with all the data is computationally impossible. The application of Eq. (19) on local patches is computationally impossible as well, because of the matrix $WC_{yy}W^T$. The problem is that the computation of $WC_{yy}W^T$ on a local patch requires to compute C_{yy} on a larger area, because the elements of the matrix $WC_{yy}W^T$ are linear combinations of the original signal covariances. In particular, since the filter kernels are generally long up to half an orbit, the computation of the matrix $WC_{yy}W^T$, even for a local patch, requires to analytically evaluate signal covariances of points covering an hemisphere. This is computationally impossible, especially if repeated for all the local patches required for the gridding.

To overcome these difficulties, an iterative space-wise approach was proposed (Migliaccio et al. 2004a), see Fig. 1. This approach is based on Wiener filtering, gridding in patches, spherical harmonic analysis by numerical integration and iterative reduction of the Wiener filter effect by the complementary filter, defined as:

$$W^c = I - W, \tag{21}$$

where I is the identity matrix. The operator W^c, even though represented with a huge matrix, can be applied spectrally in an easy numerical way because it is a time-wise convolution with the complementary kernels, defined in the frequency domain as:

$$H^c_{(i)(j)}(f) = \delta_{(i)(j)} - H_{(i)(j)}(f), \tag{22}$$

where $\delta_{(i)(j)}$ is the Kronecker delta. By means of the operator W^c the filtered data are completed by the values coming from the spherical harmonic coefficients estimated at each iteration (see Fig. 1).

The resulting iterative procedure corresponds to a complicated, yet linear, operator applied to the data. If the filter W were optimal, then by iterations there could not be any improvement by any linear operator, or, from a theoretical point of view, the application of any other linear operator, after the application of the optimal one, cannot be justified. However, there is improvement and this is because the applied filter W is not optimal, as explained in Sect. 2.2.

Here it is shown how this iterative scheme can be used to theoretically achieve the solution with respect to the Wiener–Kolmogorov principle, without the need to estimate the covariance of the estimation error after the Wiener filter. The operator S to be applied to the filtered data at every step for the estimation of spherical harmonic coefficients is considered unknown and its derivation is made so that the final estimates be optimal.

Assume a band-limited space that is described by the coefficients vector x. Then the signal y is a linear synthesis of the coefficients x represented by the matrix M. So the noisy observations are:

$$b = y + v = Mx + v. \tag{23}$$

The filtered observations at iteration zero are:

$$\hat{y}^0 = Wb = WMx + Wv. \tag{24}$$

A vector of coefficients is estimated by gridding and spherical harmonic analysis represented by the operator S:

$$\hat{x}^0 = SWMx + SWv. \tag{25}$$

The synthesis along the orbit is made so that we have a new set of "observations":

$$\hat{b}^0 = M\hat{x}^0 = MSWMx + MSWv. \tag{26}$$

Then the observations are updated according to the complementary filter scheme and new coefficients are obtained:

$$\hat{y}^1 = Wb + (I - W)\,\hat{b}^0 = Wb + (I - W)\,M\hat{x}^0, \tag{27}$$

$$\hat{x}^1 = S\hat{y}^1 = SWb + S\,(I - W)\,M\hat{x}^0. \tag{28}$$

Generalizing for any iteration n, we get:

$$\hat{y}^n = Wb + (I - W)\,M\hat{x}^{n-1}, \tag{29}$$

$$\hat{x}^n = S\hat{y}^n = SWb + S\,(I - W)\,M\hat{x}^{n-1}. \tag{30}$$

For many iterations and given that the procedure converges, i.e. that the matrix $S(I - W)M$ has norm smaller than one (Migliaccio et al. 2004a), then we get: $\hat{x}^n \equiv \hat{x}^{n-1} \equiv \hat{x}$. Therefore, Eq. (30) reads:

$$\hat{x} = (I - S\,(I - W)\,M)^{-1}\,SWb. \tag{31}$$

At this point one can impose that this estimate be equal to the theoretical optimal solution, i.e. the solution with minimum error variance for every coefficient if global collocation were numerically possible, that is:

$$\hat{x} = C_{xy}\left(C_{yy} + C_{vv}\right)^{-1} b. \tag{32}$$

Setting the two operators of Eqs. (31) and (32) equal to each other, we get:

$$\begin{aligned} &(I - S(I - W)M)^{-1}\,SW = C_{xy}\left(C_{yy} + C_{vv}\right)^{-1} \\ &\Rightarrow SW\left(C_{yy} + C_{vv}\right) = (I - S(I - W)M)\,C_{xy} \\ &\Rightarrow S\left(WC_{yy} + WC_{vv}\right) + S(I - W)C_{yy} = C_{xy}, \end{aligned} \tag{33}$$

where the following covariance propagation formula is used:

$$MC_{xy} = C_{yy}. \tag{34}$$

So we have:

$$\begin{aligned} &S\left(WC_{yy} + WC_{vv} + C_{yy} - WC_{yy}\right) = C_{xy} \\ &\Rightarrow S\left(WC_{vv} + C_{yy}\right) = C_{xy} \\ &\Rightarrow S = C_{xy}\left(C_{yy} + WC_{vv}\right)^{-1}. \end{aligned} \tag{35}$$

This is the operator that must be applied in order to obtain the theoretically optimal result.

Practically the iterative operator S is implemented by first predicting grid values z by collocation and then applying the numerical integration operator B (Eq. 16) to derive the spherical harmonic coefficients. This corresponds to rewriting Eq. (35) as:

$$S = BC_{zy}\left(C_{yy} + WC_{vv}\right)^{-1}, \tag{36}$$

where the following covariance propagation formula is used:

$$BC_{zy} = C_{xy}. \tag{37}$$

Note that, since the gridding is made in local patches of data, the applied operator S is not exactly the theoretical one (Eq. 36); therefore the final result is sub-optimal and still depends on the filter W. Note also that WC_{vv} can be computed in the frequency domain by:

$$Q_{(i)(j)}(f) = \sum_k H_{(i)(k)}(f)\,S_{v(k)v(j)}(f), \tag{38}$$

for each couple of data types i, j.

The matrix $C_{yy} + WC_{vv}$ has to be invertible (Eq. 36). Assuming that the covariance matrix C_{yy} is positive definite, a sufficient condition is that WC_{vv} is positive definite too. In order to satisfy this condition, the following approximations are implemented. First of all, smoothed noise spectra and cross-spectra are used (as already done for the Wiener filter, see Sect. 2.2), because the original noise spectra and cross-spectra can lead to a numerically non-invertible covariance

matrix C_{vv}. Then, Eq. (38) is modified:

$$\overline{Q}_{(i)(j)}(f) = \frac{Q_{(i)(j)}(f) + Q_{(j)(i)}(f)}{2} \tag{39}$$

so that the resulting WC_{vv} is symmetric. Finally, for each frequency f, the matrix composed by the elements $\overline{Q}_{(i)(j)}(f)$, with i and j the row and column indexes respectively, is forced to be positive definite by reducing by a factor α (with $0 < \alpha < 1$) the elements outside the diagonal. In this way the corresponding WC_{vv} results to be positive definite.

Typically, when filtered data are used as input to a collocation procedure, a covariance function of the error of these filtered data has to be available. Correlation between this error and the signal is commonly neglected. On the contrary, the use of the resulting operator S is very advantageous, because no error covariance function after the filtering has to be estimated, nor any correlation of signal with error after filtering has to be modelled. This property can be used in any step-wise collocation procedure.

The assumption that the vector x is finite is not necessary for the derivation of Eq. (35). Since the coefficient estimates converge to zero for increasing degree, because of the regularization imposed by collocation, the synthesis operator M can be applied up to a certain maximum degree and be reasonably considered as an infinite operator. Then the operator M is also propagated to covariances (Eq. 34), which can be computed up to infinite degree with closed expressions of converging degree variance series (Tscherning and Rapp 1974).

The assumption that the vector x is finite is however necessary for the derivation of Eq. (36). In fact, both Eqs. (36) and (37) hold only if Eq. (15) can be inverted, i.e. $A^T A$ is invertible (see Eq. 16). Since the vector z is finite, a necessary condition to invert Eq. (15) is that the vector x is finite too and $\dim(x) \leq \dim(z)$ (Reguzzoni et al. 2006). Since in reality x is infinite, then there is aliasing and loss of information. However, at satellite altitude above a certain spherical harmonic degree (e.g. 360), the power of the signal is not significant with respect to the noise level, so that the high-degree information is practically cancelled out by the collocation gridding. Therefore, a proper choice of $\dim(z)$, i.e. of the grid resolution, can significantly reduce aliasing. Again it has to be noted that loss of information is also present because of the patch-wise gridding.

3.3 Iterative solution with rotation corrections

In this section, the multi-step optimal operator (Eq. 35) is revised by taking into account that the gravity gradient tensor is measured in the Gradiometer Reference Frame (GRF), which is slightly different from LORF. GRF is known to oscillate, i.e. it is moving almost periodically, and this could have a negative effect in terms of stationarity of the signal (Migliaccio et al. 2006). Also, it is numerically much more convenient to perform the gridding in LORF than in GRF, because LORF is closer to the local East North Up (ENU) frame and the signal covariances for second-order derivatives are first derived in ENU and then rotated to the considered frame (Tscherning 1993).

The original observations, i.e. the gravity gradients in GRF, are now denoted as:

$$g = Gx + \varepsilon, \tag{40}$$

where the operator G represents the synthesis of all six gravity gradients in GRF and ε is the original observation noise. The corresponding gravity gradients l in LORF are:

$$l = Rg = RGx + R\varepsilon, \tag{41}$$

where R is the rotation matrix from GRF to LORF. Since two of the off-diagonal gravity gradients are known to be very noisy, the rotation matrix R would spread their noise onto all gravity gradients. For this reason, the elements of the matrix R acting on the very noisy gravity gradients are forced to zero, obtaining a new matrix denoted by R_1. The ignored terms are assembled in another matrix, denoted by R_2, so that:

$$R = R_1 + R_2. \tag{42}$$

Note that the elements of R_2 are small, because the two frames GRF and LORF are close to each other, however, they are not equal to zero and their effect cannot be completely neglected (Migliaccio et al. 2006).

The matrix M for the synthesis of all gravity gradients in LORF can be divided into two parts as well, i.e.:

$$M = RG = R_1 G + R_2 G = M_1 + M_2. \tag{43}$$

Since only the incomplete rotation R_1 is applied to the gravity gradients in GRF, the actually used observations are:

$$b = R_1 g = M_1 x + v, \tag{44}$$

where now the noise v is:

$$v = R_1 \varepsilon. \tag{45}$$

In order to account for the missing part, at every iteration n the rotation correction term $M_2 \hat{x}^{n-1}$ is added to the filtered data $\hat{y}^n$ in Eq. (29), where also M_1 is used instead of M. So the new solution, given that there is convergence, is like Eq. (31), with the further term SM_2:

$$\hat{x} = (I - S(I - W)M_1 - SM_2)^{-1} SWb. \tag{46}$$

At this point, the optimal global solution is Eq. (32) with $C_{xy} = C_{xx} M_1^T$ and $C_{yy} = M_1 C_{xx} M_1^T$. Setting the operators of Eqs. (46) and (32) equal to each other and applying

simplifications (like in the previous derivation), we get:

$$S = C_{xy}\left(C_{yy} + M_2 C_{xy} + WC_{vv}\right)^{-1}$$
$$= C_{xy}\left((M_1 + M_2)C_{xx}M_1^T + WC_{vv}\right)^{-1}. \quad (47)$$

Note that the difference of this solution with respect to Eq. (35) is the term $M_2 C_{xy}$. However the signal covariance matrix $M_1 C_{xx} M_1^T$ is very difficult to compute, because M_1 corresponds to a functional of the gravitational potential that has no clear physical meaning. Therefore, in practice, the operator S is implemented as follows:

$$S = C_{xx}(M_1 + M_2)^T \times \left((M_1 + M_2)C_{xx}(M_1 + M_2)^T + WC_{vv}\right)^{-1}$$
$$= C_{xx}M^T\left(MC_{xx}M^T + WC_{vv}\right)^{-1}, \quad (48)$$

where the use of the matrix M corresponds to considering the input data to the operator S as gravity gradients in LORF (Eq. 43). Since LORF differs from the ENU frame by only one rotation around the Up axis, this means that computing the covariances of Eq. (48) is feasible (Tscherning 1993). Note that for $M_2 \equiv 0$ then Eqs. (47) and (48) are the same. However this is a deviation of the implemented method from the theoretical optimal solution.

4 Numerical experiments

4.1 Test data description

A time-series of sixty days of simulated realistic GOCE data is used for numerical tests. The observations of this time-series are corrupted by realistic in-flight calibration noise (Catastini et al. 2007). The signal is based on EGM96 (Lemoine et al. 1998) up to degree and order 360.

First the gravitational potential is estimated by the energy conservation method, using the satellite positions and velocities, as well as the non-gravitational accelerations measured by the accelerometers of the gradiometer. A calibration procedure is implemented (Migliaccio et al. 2007a) so that simulated biases in the non-gravitational accelerations measurements are removed. From the potential data, a spherical harmonic model up to degree and order 50 is created by collocation gridding in patches and then numerical integration, i.e. the two-step procedure. The observational functionals, namely the gravity gradients and the potential, are computed from this reference model and subtracted from the data so that the long wavelength effects are largely removed. Then the gravity gradients are calibrated for trends by spline interpolation (Migliaccio et al. 2007a). These reduced and calibrated data are then used for the subsequent processing steps. A flow-chart of this data pre-processing step is shown in Fig. 2. Error statistics are reported in Table 2.

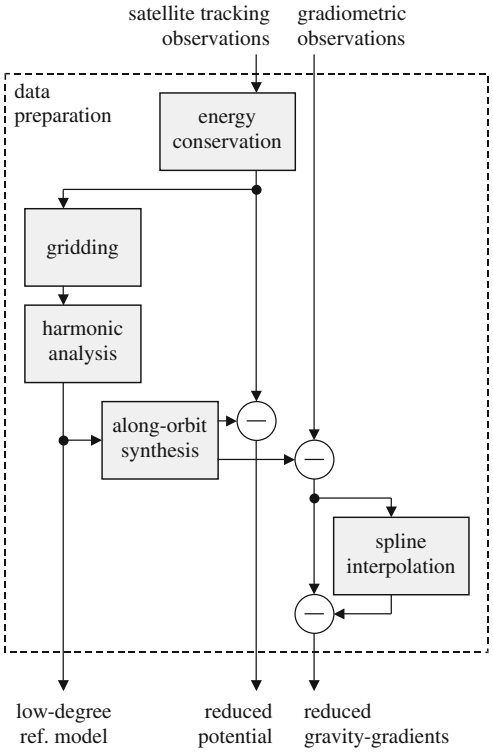

Fig. 2 Flow-chart of the data pre-processing and of the low-degree reference model computation

Table 2 Noise standard deviation of the observations, i.e. the potential T obtained from energy conservation (units are m^2s^{-2}) and the gravity gradients after the calibration (units are Eötvös = $10^{-9}s^{-2}$)

Data type	Noise std
T	1.6026
$T_{\xi\xi}$	0.1356
$T_{\xi\eta}$	0.2715
$T_{\xi r}$	0.0897
$T_{\eta\eta}$	0.0952
$T_{\eta r}$	0.3604
T_{rr}	0.1202

4.2 Noise covariance estimation

For the Wiener filter application, the signal and noise power spectra, i.e. the Fourier transforms of the corresponding covariance functions, are needed (Eq. 9). The signal power spectra are approximated empirically (Blackman and Tukey 1958) by the values obtained from an a-priori model, e.g. the EIGEN-GL04C model (Förste et al. 2007), to which the reference model up to degree and order 50 has been previously subtracted. The signal plus noise power spectra is empirically computed by using the values of the observations (Migliaccio et al. 2006). However, when an a-priori model is used to approximate the signal power spectrum, then it is

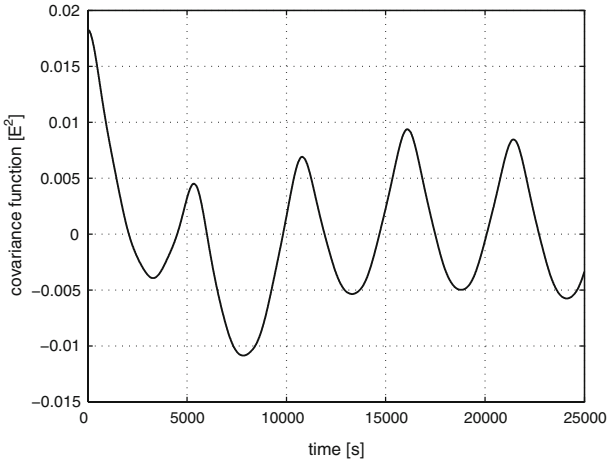

Fig. 3 True noise covariance function of $T_{\xi\xi}$. The approximation from the a-priori model at this scale is practically overlapped. E = Eötvös (10^{-9}s^{-2})

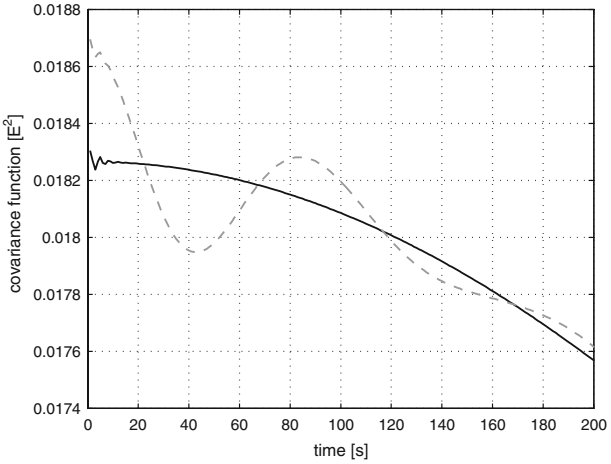

Fig. 5 True noise covariance function of $T_{\xi\xi}$ (*solid black line*). At this zoomed view, the difference of the approximated noise covariance (*grey dashed line*) is visible

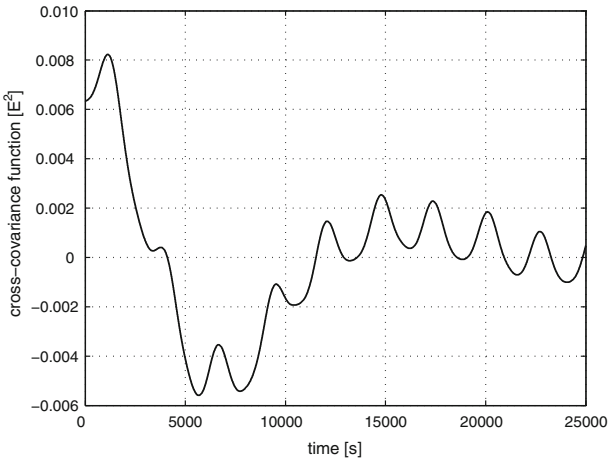

Fig. 4 True noise cross-covariance function of $T_{\xi\xi}$ and T_{rr}. The approximation from the a-priori model at this scale is practically overlapped

explicitly assumed in the Wiener filter that the noise power spectrum is equal to the power spectrum of the observations minus the power spectrum from the a-priori model. This is done also for power cross-spectra.

In order to improve the quality of this approximation, the trace of the observed gravity-gradient tensor, i.e. the sum of the diagonal components of the tensor, is computed. This sum is different from zero because of the observation noise and this can be used to calibrate the estimated power spectra and cross-spectra. In particular, the power spectrum of the trace error can be computed empirically from the data and, also, derived by propagation from the estimated noise power spectra and cross-spectra. By demanding that the propagated power spectrum is equal to the empirical one, a scale factor for each frequency f can be determined. These scale factors are then applied to all the estimated noise power spectra and cross-spectra.

This approximation turns out to be of sufficient quality for our purposes, for both power spectra and power cross-spectra, as shown in Figs. 3, 4 and 5. Here the EIGEN-GL04C model is used as an a-priori model, which is different from EGM96. Note that the modelled noise refers to Eqs. (44) and (45).

A flow-chart of this estimation procedure is displayed in Fig. 6. Its main advantage is that noise covariances and cross-covariances for all the data types are estimated. In this way all the available data, including off-diagonal second order derivatives, can be used in the gravity field processing. The modelled C_{vv} can be also used for error propagation purposes with, for instance, Monte–Carlo methods (Alkhatib and Schuh 2007) and this is dealt with in Migliaccio et al. (2007c).

4.3 Wiener filter implementation and results

According to Sect. 2.2, the signal and the observations (signal plus noise) power spectra have to be modified for the Wiener filter application (Fig. 7) so that the corresponding covariance functions get zero after a short time interval. The power spectra are thus convolved by a taper cosine function (Blackman and Tukey 1958) so that the resulting power spectra are smoothed. The length of this function, and thus the time interval after which the covariances get zero, has to be chosen. The Wiener filter is applied and the trace error of the filtered data is computed. This is repeated by using taper cosine functions of different length and a selection based on the minimum trace error variance is made. It results that the window chosen, for varying filter combinations (i.e. varying index set J of Eq. 2) and for varying data intervals (the whole sixty days of data or smaller parts), is always such

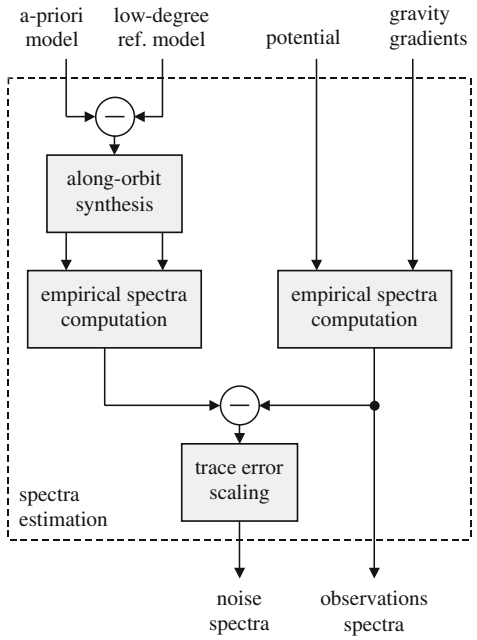

Fig. 6 Flow-chart of the power spectra estimation of the noise and of the observations

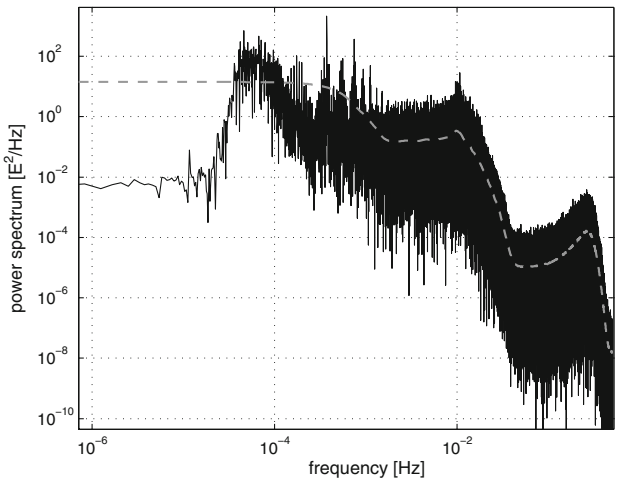

Fig. 7 Empirical power spectrum of T_{rr} observations (*black*) and the corresponding smoothed power spectrum (*grey dashed*). The low values at the beginning of the empirical power spectrum (*black*) are due to the splines calibration (Migliaccio et al. 2007a)

that the resulting covariances vanish at around one quarter of an orbit (Fig. 8). This is expected from the considerations made in Sect. 2.2. Anyway, the window length is not a critical parameter, in the sense that the results of the filtering are almost the same even for a window with double or half the optimal length.

Error statistics of the filtered data are reported in Table 3. Two filtering scenarios are considered. In the first scenario, one-input data (1D) filters are used, according to Eq. (10). In the second scenario, two-input data (2D) filters are used,

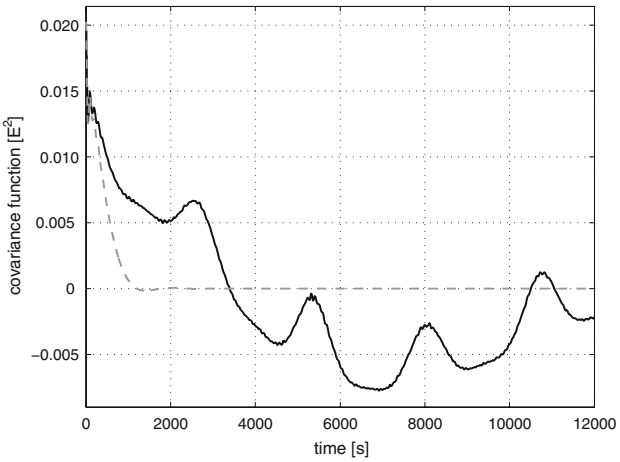

Fig. 8 Covariance function of T_{rr} observations (*black*) and the corresponding covariance function after smoothing the power spectrum (*grey dashed*). The covariance function gets zero at about 1,300 s, that is close to a quarter of 5,300 s (i.e. one GOCE orbit)

Table 3 Estimation error standard deviation of the filtered observations, i.e. the potential T (units are m^2s^{-2}) and the gravity gradients (units are Eötvös = $10^{-9}s^{-2}$), for 1D and 2D filters

Data type	Error std 1D	Error std 2D
T	0.0487	0.0438
$T_{\xi\xi}$	0.0020	0.0018
$T_{\xi\eta}$	0.0138	0.0138
$T_{\xi r}$	0.0030	0.0030
$T_{\eta\eta}$	0.0081	0.0044
$T_{\eta r}$	0.0283	0.0283
T_{rr}	0.0097	0.0046

by also exploiting the potential for the filtering of the gravity gradients and the second radial derivatives T_{rr} for the filtering of the potential. This means that the index set J of Eq. (2) is equal to $\{i, 0\}$ for the gravity gradients, i.e. for $i = 1, 2, \ldots 6$, while J is equal to $\{0, 6\}$ for the potential. In this way, the low-frequency content of the gravity gradients that is dominated by noise (Migliaccio et al. 2006) is corrected by using the potential and vice versa. Note that any combination is possible, since every data type i is treated independently from the other data types. For example T is used to filter $T_{\xi\xi}$, but $T_{\xi\xi}$ is not used to filter T.

Some comments are due on the choice of the filtering scenario. It is numerically verified that 2D filters lead to a singular matrix W, while 1D filters do not. This happens because the information of the potential dominates at low frequencies, where the gravity gradients measurements are very noisy. This causes the 2D filtering to cancel those frequencies of the gravity gradients and use only the information of the potential, i.e. a projection to a smaller space is made. Since the matrix W is not invertible (and not even symmet-

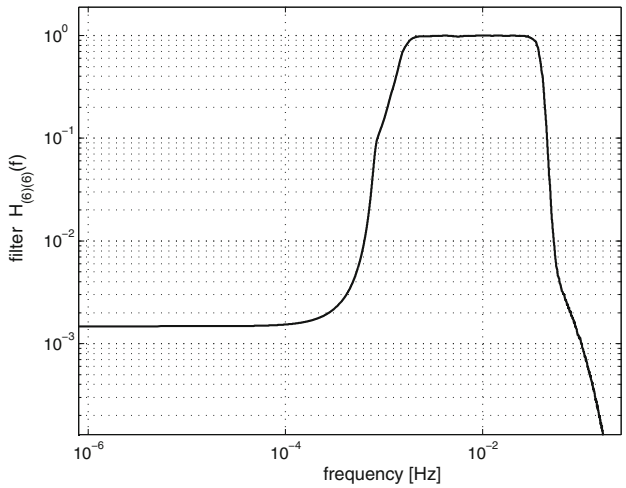

Fig. 9 The filter $H_{(6)(6)}(f)$ applied to T_{rr}. It can be seen that the filter is equal to 1 where the signal dominates (see Fig. 10)

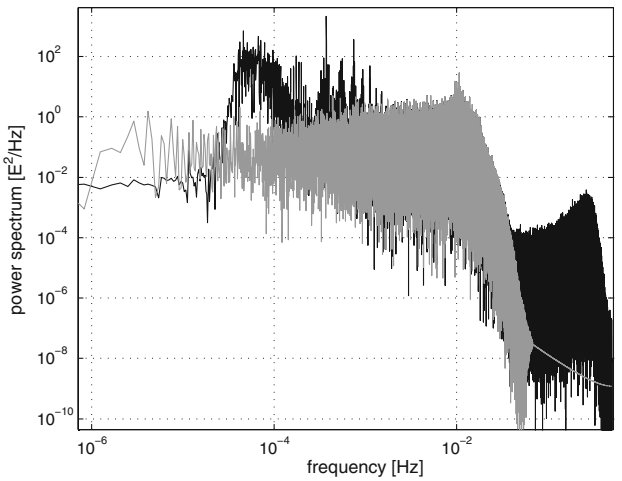

Fig. 10 Time-wise power spectrum of the T_{rr} observations (*black*, same as Fig. 7) and a-priori time-wise power spectrum of the T_{rr} signal (*grey*). It can be seen that at some frequencies the signal power spectrum is as high as that of the observations. This means that at those frequencies the noise is low and the signal dominates

ric), then the matrix WC_{vv} must be regularized as explained in Sect. 3.2, while this regularization is not necessary in the case of 1D filters. This is an argument to choose the 1D filtering, although this argument is not definitive, since the optimal solution is not achieved anyway because of the gridding in patches. On the other hand, when 2D filters are used, the filtered data have a higher accuracy (see Table 3), thus implying the choice of 2D filters. A final decision should depend on the accuracy of the estimated spherical harmonic coefficients at the end of the multi-step procedure. From the experiments performed, which are not reported here for brevity, the 2D filters perform slightly better in the majority of the cases and therefore these filters are used in the sequel.

As an example, the computed function $H_{(6)(6)}(f)$ (see Eq. 9) is shown in Fig. 9. The filter acts like a scale factor in the frequency domain, i.e. it is close to 1 at those frequencies where the signal dominates (Fig. 10), otherwise it approaches to zero. The filter does not consider the oscillations of the power spectra because of the used smoothing window. In terms of time covariances, this means that the filter is not adapted to the long period oscillations of the noise covariance function (see Figs. 3 and 4).

4.4 Gridding implementation

A unique global signal covariance function is used for the gridding, based on a finite number of degree variances, up to degree 360, which is the same maximum degree used in the simulation of the test data. The covariances are modelled by series of Legendre polynomials (Tscherning 1976a,b). The potential is used together with the gravity gradients and therefore the derivation of the cross-covariances between potential and gravity gradients in a rotated reference frame is needed (Tscherning 1993). The degree variances used are those coming from EGM96 minus the reference model up to degree 50. The problem of estimating degree variances from data is not considered here; the related issue of global or local signal covariance modelling is not addressed either.

In principle, the noise covariance functions estimated as described in Sect. 4.2 should be used for the gridding. As a matter of fact, the corresponding covariance matrix C_{vv} is not invertible, even for a local patch. This is mainly due to the very long correlation of the gradiometer noise. For this reason, the noise covariance functions are derived from the smoothed noise power spectra (the same already used for the Wiener filter).

Two different spherical grids at mean satellite altitude are computed, namely one for T and one for T_{rr}, because they give rise to different results in terms of spherical harmonic coefficient estimates (Migliaccio et al. 2007b). These estimates are then combined with weights determined from the error degree variances, though their optimal combination is still an open issue and can be achieved by full error covariance matrix estimation.

The size of the patches of data for the local gridding is $6^\circ \times 6^\circ$ with 2° of overlap; this choice is a trade-off between the number of data contained in the patch and the time required for the collocation solution. The overlap is necessary to reduce the discontinuities among different patches. The grid resolution is 0.2° in both latitude and longitude; with such a high resolution, discretization errors of the spherical harmonic analysis by numerical integration are negligible.

As input to the gridding procedure the potential T and the four most accurate gravity gradients, namely $T_{\xi\xi}$, $T_{\xi r}$, $T_{\eta\eta}$ and T_{rr} (see Table 3), are jointly used. The two less accurate gravity gradients, $T_{\xi\eta}$ and $T_{\eta r}$, are not used because the time

needed to obtain a solution including these two components increases, but the accuracy of the solution does not improve at all.

A decimation before the gridding is applied, i.e. only one out of twelve observations is used; this makes the solution much faster. In order to obtain a more homogeneous spatial distribution, a higher sampling rate is considered in the equatorial area, where the data are less dense. In fact, it is demonstrated that a proper data distribution can improve spherical harmonic coefficient recovery (Arabelos and Tscherning 2007).

Due to the orbit inclination of the GOCE satellite (about 96.5°) the polar caps are not covered with data. In Migliaccio et al. (2007a), grid values on the polar caps were extrapolated and the results were of good quality, in terms of controlling the error of the low-order coefficients. These coefficients are those mainly affected by missing data at the poles (Sneeuw and van Gelderen 1997). In fact, covering all the sphere with data is required so that a relation like Eq. (16) is numerically well-defined for the low-order coefficients as well. Otherwise the matrix $A^T A$ in Eq. (16) would have eigenvalues close to zero. Note that since the extrapolation is realized by collocation, then the finally resolved coefficients correspond to approximating the global collocation solution using the original observations (Eq. 13). In any case, the estimated low-order coefficients are inevitably of poor quality.

4.5 Two-step solution versus iterative multi-step solution

First a direct gridding (with patches as defined in Sect. 4.4) without applying the Wiener filter and without any iterations is performed. Spherical harmonic coefficients are then estimated by numerical integration. This procedure corresponds to the two-step solution (see Sect. 3.1) and leads to a geoid commission error of 27.0 cm up to degree and order 200 in the latitude interval from −80° to 80° (Fig. 11).

Then the gravity field solution is performed with the Wiener filter and iterations according to Sect. 3.2 and Sect. 3.3. The 2D filters defined in Sect. 4.3 are used. The geoid error up to degree and order 200 inside the latitude interval from −80° to 80° at iteration zero is 10.5 cm. After four iterations, the error decreases to 5.6 cm (Fig. 12). This result is a numerical justification of the use of the Wiener filter.

The flow-chart of the implemented two-step solution is shown in Fig. 13, while the one of the iterative multi-step solution is shown in Fig. 14.

Note that the spherical harmonic coefficients estimated by numerical integration are not regularized, in the sense that the error power goes beyond the signal power at high degrees (Fig. 15). This happens because the gridding by collocation is performed in patches (Migliaccio et al. 2007b) and it is corrected by a posterior combination of the estimated model with a set of spherical harmonic coefficients all equal to zero, i.e. with error degree variances equal to the signal degree variances. This produces a regularization, just like collocation.

The two tests are repeated. Now a reference model for the high degrees is subtracted, i.e. the EIGEN-GL04C model is removed from degree 51 to 360. Signal covariance is recomputed according to the residual degree variances. The application of the two-step solution (see Fig. 13) results to a commission geoid error of 12.8 cm for a solution up to degree and order 200 in the latitude interval from −80° to 80° (Fig. 16).

On the other hand, when the multi-step solution with the Wiener filter is used (see Fig. 14), the geoid error at iteration zero is 5.2 cm. After four iterations the error drops to 4.2 cm (Fig. 17). This confirms that the Wiener filter is useful even when a reference model is subtracted. The difference of the two solutions is also visible when the error degree variances are compared (Fig. 18).

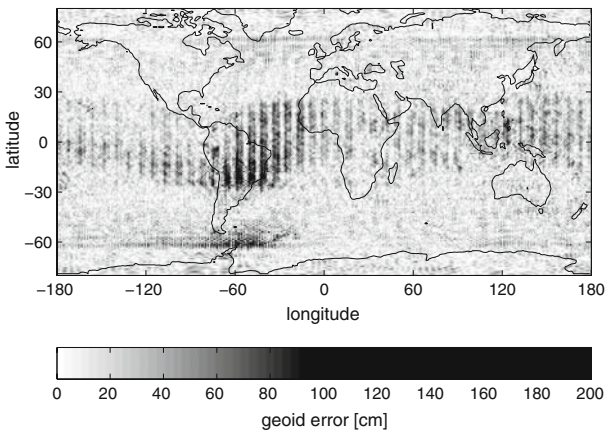

Fig. 11 Geoid error (degree & order 200), computed without the Wiener filter

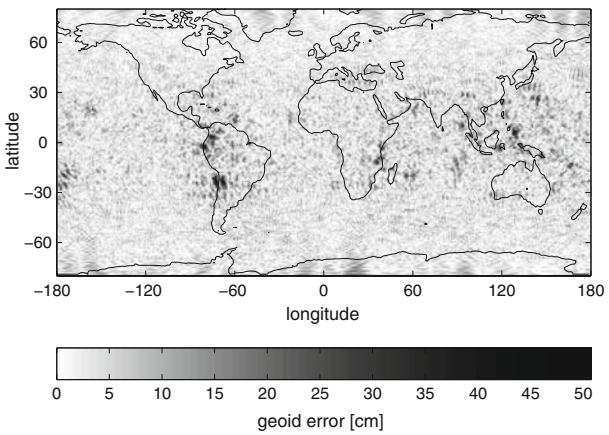

Fig. 12 Geoid error (degree & order 200), computed with the Wiener filter and with the optimal iterative operator

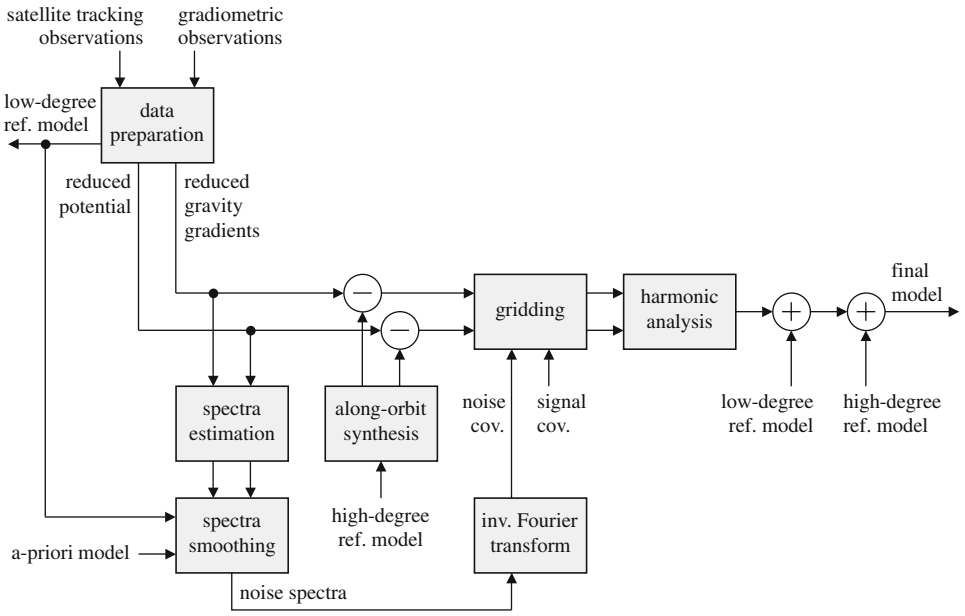

Fig. 13 Flow-chart of the implemented two-step solution. The blocks called as "data preparation" and "spectra estimation" are described in details in Figs. 2 and 6, respectively. The use of the high-degree reference model is optional

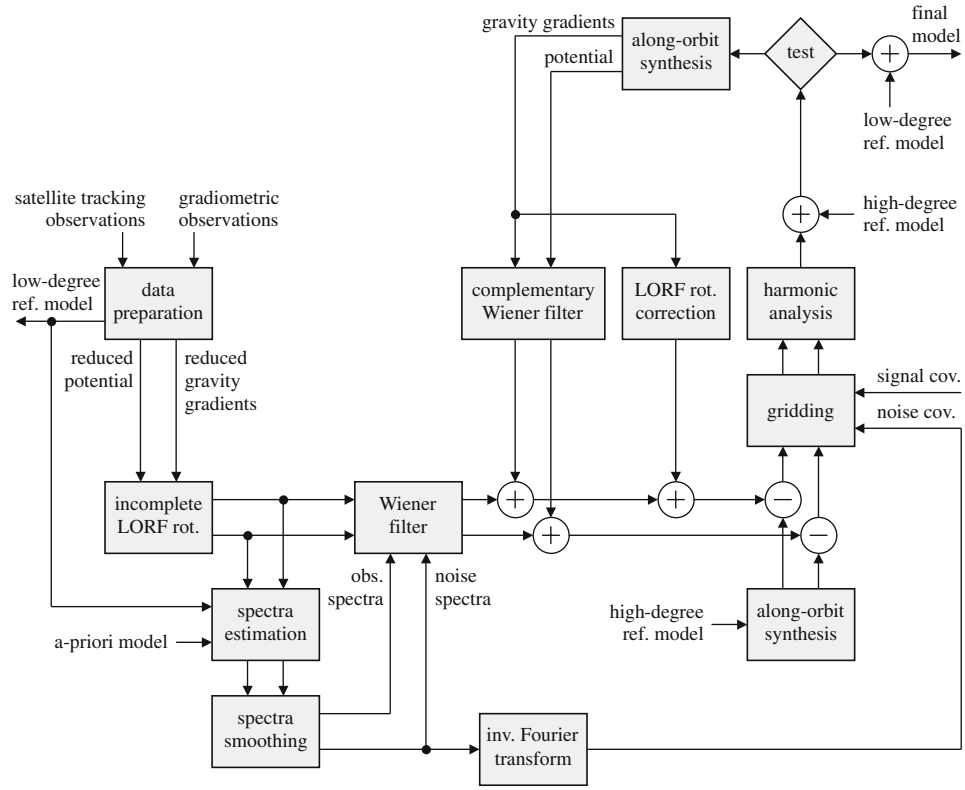

Fig. 14 Flow-chart of the implemented iterative multi-step solution. The blocks called as "data preparation" and "spectra estimation" are described in details in Figs. 2 and 6, respectively. The use of the high-degree reference model is optional

Regarding the spatial distribution of the geoid error, the two-step solution is characterized by significant features with a regular pattern covering large areas (see Figs. 11, 16). These features are related to the long correlations (both of signal and noise) that are not considered when only gridding in patches is performed. The use of the Wiener filter before the gridding, in the framework of the iterative multi-step procedure, allows to eliminate these error features (see Figs. 12, 17). The remaining error shows a clear topographic signature, e.g. with higher values in the Himalayas or in the Andes (see Fig. 17). This effect is characteristic of collocation methods because the estimation error is correlated with the signal.

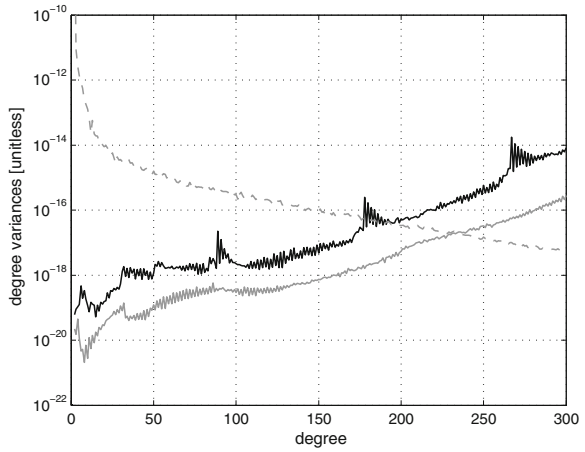

Fig. 15 Error degree variances of the solutions computed with (*grey*) and without (*black*) the Wiener filter. The signal degree variances of EGM96 are in *dashed grey*

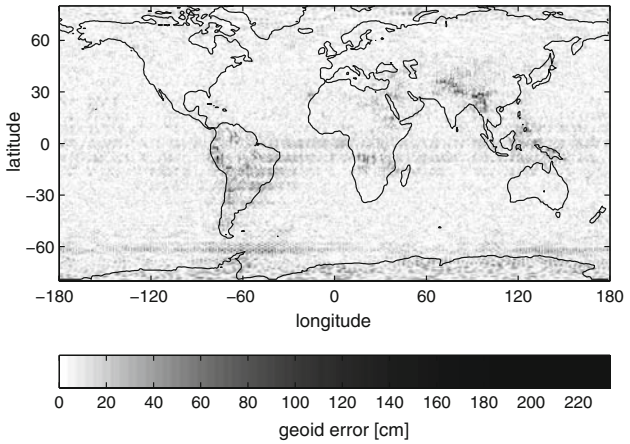

Fig. 16 Geoid error (degree & order 200), using EIGEN-GL04C as reference model, without the Wiener filter

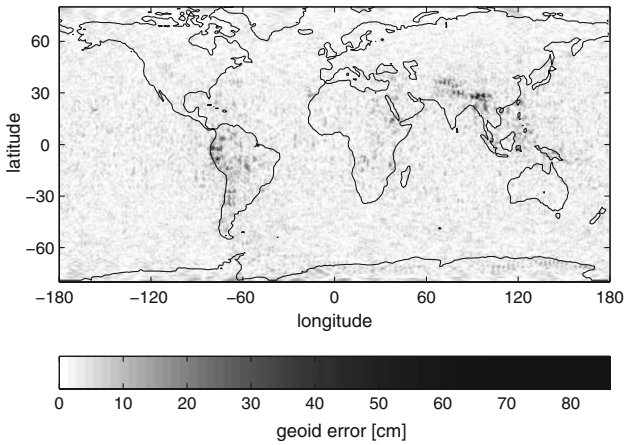

Fig. 17 Geoid error (degree & order 200), using EIGEN-GL04C as reference model, with the Wiener filter and with the optimal iterative operator

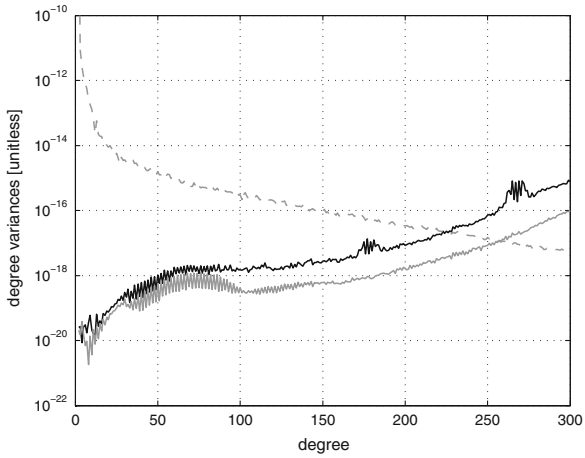

Fig. 18 Error degree variances of the solutions using EIGEN-GL04C as reference model, with (*grey*) and without (*black*) the Wiener filter. The signal degree variances of EGM96 are in *dashed grey*

4.6 A-priori model and reference model iterations

The noise power spectra estimation and calibration with the trace error is repeated (see Sect. 4.2), but now the model computed with the Wiener filter and EIGEN-GL04C as reference is used, instead of an a-priori model. The improvement is significant (see Fig. 19). The reference model that is removed from the data before the gridding is also updated: a synthesis of a grid of the gravitational potential, again from the model estimated with the Wiener filter and EIGEN-GL04C, is computed at ground level (so that no downward continuation problems arise). Then the peaks of this grid are statistically selected, some smoothing is applied (for preventing Gibbs effects) and finally a spherical harmonic analysis by numerical integration is performed; see Migliaccio et al. (2004b) for details. In this way, a reference model describing the inhomogeneities of the gravitational field is obtained. By using the new noise spectra and the new reference model, the accuracy of the resulting space-wise solution at the end of the iterative multi-step procedure is 2.6 cm of geoid error.

The noise power spectra estimation and calibration is performed for a third time (without significant improvement), the peaks reference model is computed again and the space-wise solution now gives rise to a geoid error of 2.4 cm (Fig. 20). The small improvement is due to the better homogeneity of the residual field. Note that over the whole sphere the error is 17.2 cm due to the polar gap effects (Fig. 21).

In these tests the convergence of the iterative multi-step procedure (Fig. 14) is fast, i.e. three iterations lead to below 0.1 mm difference in geoid heights between the last two solutions.

The computer used to perform these numerical experiments is a 3 GHz bi-processor with 4 GB RAM. The time required for each processing of the sixty day data set with

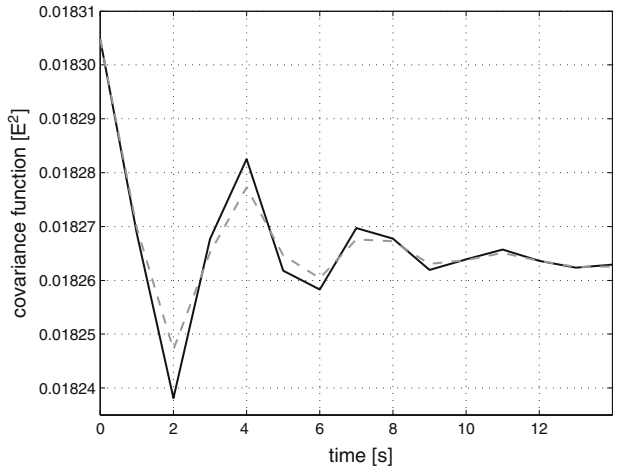

Fig. 19 True noise covariance function of $T_{\xi\xi}$ (*solid black line*) and its approximation based on the estimated model instead of EIGEN-GL04C (*grey dashed line*). Notice the different scale compared to Fig. 5

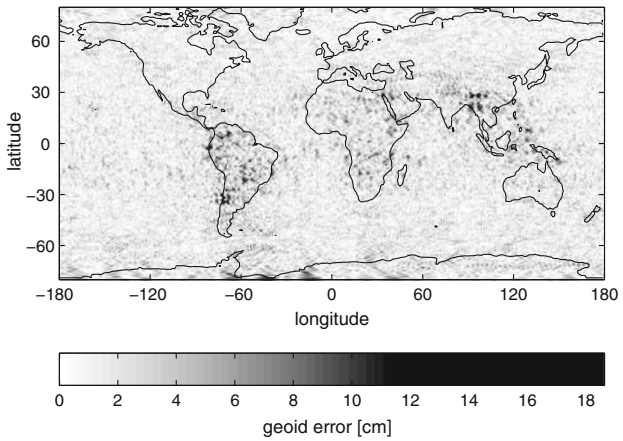

Fig. 20 Geoid error (degree & order 200), using an improved reference model, with the Wiener filter and with the optimal iterative operator

the iterative scheme of Fig. 14, performing three or four iterations to reach convergence, is about three days. In this sense the method can be considered numerically efficient.

5 Conclusions and outlook

The space-wise approach for GOCE data analysis is a multi-step collocation technique. It comprises the Wiener filter, gridding by collocation, spherical harmonic analysis by numerical integration; all the steps are applied iteratively. The scope of this work is the theoretical optimization of this multi-step collocation technique, which is achieved in a way that it is also, to some extent, numerically applicable. The logical scheme used to optimize the space-wise approach can be applied to any kind of step-wise collocation procedure.

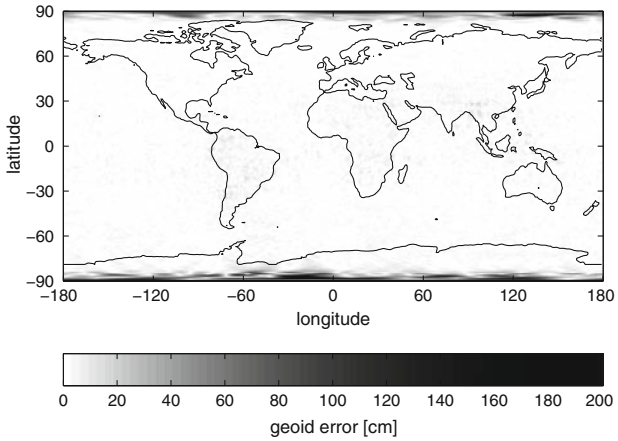

Fig. 21 Geoid error (degree & order 200), using an improved reference model, with the Wiener filter and with the optimal iterative operator. Over the whole sphere the error at the poles dominates

The complexity of the space-wise approach is due to the Wiener filter. This filter is a fast time-wise collocation. However, it is seen that the signal covariance functions are poorly approximated. Therefore, this filter is not optimal and its error estimates are not consistent. A modification is made so that the filter is valid for short time periods only. Then, the original plan of the space-wise approach is revised in such a way that the iterative scheme based on the complementary Wiener filter is equivalent to the direct collocation solution, i.e. to the optimal solution according to the Wiener–Kolmogorov principle. This is proved theoretically, however some approximations are needed for numerical reasons, like performing the gridding in patches, and therefore the final solution is only sub-optimal. The convergence of the implemented iterative scheme is tested numerically.

Experiments on simulated GOCE data are performed to assess the impact of the Wiener filter in a collocation procedure to estimate spherical harmonic coefficients of the gravitational potential. Since the gridding by collocation is applied inside limited patches of data, the long correlation of the noise cannot be handled. This is the main reason why the tapering of the Wiener filter is useful. The better performance of the collocation solution when the Wiener filter is used, compared to the solution without the filter, is verified numerically in terms of accuracy of the recovered spherical harmonic coefficients and accuracy of the computed geoid.

The general remark is that any step-wise procedure should be studied so that it leads to a well-defined solution based on optimality criteria. In particular, any step-wise collocation method should be based on two principles: to model the statistical characteristics of the data as good as possible and apply the Wiener–Kolmogorov principle as accurately as possible.

Acknowledgments This work was performed under ESA contract No. 18308/04/ NL/NM (GOCE High-level Processing Facility). The authors wish to thank Prof. Sansò for the fruitful discussions and the reviewers for their comments and suggestions.

References

Albertella A, Migliaccio F, Reguzzoni M, Sansò F (2004) Wiener filters and collocation in satellite gradiometry. In: Sansò F (ed) International association of geodesy symposia, "V Hotine–Marussi symposium on mathematical geodesy", 17–21 June 2002, Matera, Italy, vol 127. Springer, Berlin, pp 32–38

Alkhatib H, Schuh WD (2007) Integration of the Monte Carlo covariance estimation strategy into tailored solution procedures for large-scale least squares problems. J Geod 81:53–66. doi:10.1007/s00190-006-0034-z

Andritsanos VD, Sideris MG, Tziavos IN (2001) Quasi-stationary sea surface topography estimation by the multiple input/output method. J Geod 75:216–226. doi:10.1007/s001900100169

Arabelos D, Tscherning CC (2007) On a strategy for the use of GOCE gradiometer data for the development of a geopotential model by LSC. In: Proceedings of the 3rd international GOCE user workshop, 6–8 November 2006, Frascati, Italy (ESA SP-627, January 2007), pp 69–75. ISBN 92-9092-938-3, ISSN 1609-042X

Basilevsky A (1983) Applied matrix algebra in the statistical sciences. Dover Publications, New York

Blackman RB, Tukey JW (1958) The measurement of power spectra from the point of view of communications engineering. Dover Publications, New York

Bouman J, Rispens S, Koop R (2007) GOCE gravity gradients for use in Earth sciences. In: Proceedings of the 3rd international GOCE user workshop, 6-8 November 2006, Frascati, Italy, (ESA SP-627, January 2007), pp 135–139. ISBN 92-9092-938-3, ISSN 1609-042X

Bronshtein IN, Semendyayev KA, Musiol G, Muehlig H (2004) Handbook of mathematics. Springer, Berlin

Bruinsma S, Marty JC, Balmino G (2004) Numerical simulation of the gravity field recovery from GOCE mission data. In: Proceedings of the 2nd international GOCE user workshop, 8–10 March 2004, Frascati, Italy, (ESA SP-569, June 2004). ISBN 92-9092-880-8, ISSN 1609-042X

Catastini G, Cesare S, De Sanctis S, Dumontel M, Parisch, Sechi G (2007) Predictions of the GOCE in-flight performances with the end-to-end system simulator. In: Proceedings of the 3rd international GOCE user workshop, 6–8 November 2006, Frascati, Italy, (ESA SP-627, January 2007), pp 9–16. ISBN 92-9092-938-3, ISSN 1609-042X

Colombo OL (1981) Numerical methods for harmonic analysis on the sphere. Report No. 310, Department of Geodetic Science and Surveying, Ohio State University, Columbus

Drinkwater RM, Haagmans R, Muzi D, Popescu A, Floberghagen R, Kern M, Fehringer M (2007) The GOCE gravity mission: ESA's first core Earth explorer. In: Proceedings of the 3rd international GOCE user workshop, 6–8 November 2006, Frascati, Italy, (ESA SP-627, January 2007), pp 1–7. ISBN 92-9092-938-3, ISSN 1609-042X

ESA (1999) Gravity field and steady-state ocean circulation mission. ESA SP-1233 (1). ESA Publication Division, c/o ESTEC, Noordwijk

Förste Ch, Flechtner F, Schmidt R, König R, Meyer U, Stubenvoll R, Rothacher M, Barthelmes F, Neumayer H, Biancale R, Bruinsma S, Lemoine JM, Loyer S (2007) Global mean gravity field models from combination of satellite mission and altimetry/gravimetry surface data. In: Proceedings of the 3rd international GOCE user workshop, 6–8 November 2006, Frascati, Italy, (ESA SP-627, January 2007), pp 163–167. ISBN 92-9092-938-3, ISSN 1609-042X

Gruber T, Rummel R, Koop R (2007) How to use GOCE level 2 products. In: Proceedings of the 3rd international GOCE user workshop, 6–8 November 2006, Frascati, Italy (ESA SP-627, January 2007), pp 205–211. ISBN 92-9092-938-3, ISSN 1609-042X

Jekeli C (1998) Error analysis of padding schemes for DFT's of convolutions and derivatives. Report No. 446, Department of Civil and Environmental Engineering and Geodetic Science, The Ohio State University, Columbus

Jekeli C (1999) The determination of gravitational potential differences from satellite-to-satellite tracking. Celestial Mech Dyn Astron 75:85–101

Klees R, Ditmar P, Broersen P (2003) How to handle colored observation noise in large least-squares problems. J Geod 76:629–640. doi:10.1007/s00190-002-0291-4

Lemoine FG, Kenyon SC, Factor JK, Trimmer RG, Pavlis NK, Chinn DS, Cox CM, Klosko SM, Luthcke SB, Torrence MH, Wang YM, Williamson RG, Pavlis EC, Rapp RH, Olson TR (1998) The development of the joint NASA GSFC and NIMA geopotential model EGM96, NASA Tech Rep, 1998-206861, Greenbelt

Migliaccio F, Reguzzoni M, Sansò F (2004a) Space-wise approach to satellite gravity field determination in the presence of coloured noise. J Geod 78:304–313. doi:10.1007/s00190-004-0396-z

Migliaccio F, Reguzzoni M, Sansò F, Tscherning CC (2004b) The performance of the space-wise approach to GOCE data analysis, when statistical homogenization is applied. Newton's Bull 2:60–65

Migliaccio F, Reguzzoni M, Tselfes N (2006) GOCE: a full-gradient simulated solution in the space-wise approach. In: Tregoning P, Rizos C (eds) International association of geodesy symposia, "dynamic planet—monitoring and understanding a dynamic planet with geodetic and oceanographic tools", IAG2005 - Scientific Assembly, 22–26 August 2005, Cairns, Australia, vol 130. Springer, Berlin, pp 383–390

Migliaccio F, Reguzzoni M, Sansò F, Tselfes N, Tscherning CC, Veicherts M (2007a) The latest of the space-wise approach for GOCE data analysis. In: Proceedings of the 3rd international GOCE user workshop, 6–8 November 2006, Frascati, Italy (ESA SP-627, January 2007), pp 241–248. ISBN 92-9092-938-3, ISSN 1609-042X

Migliaccio F, Reguzzoni M, Sansò F, Tselfes N (2007b) On the use of gridded data to estimate potential coefficients. In: Proceedings of the 3rd international GOCE user workshop, 6–8 November 2006, Frascati, Italy (ESA SP-627, January 2007), pp 311-318. ISBN 92-9092-938-3, ISSN 1609-042X

Migliaccio F, Reguzzoni M, Sansò F, Tselfes N (2007c) An error model for the GOCE space-wise solution by Monte Carlo methods. In: Proceedings of the XXIV IUGG general assembly, 2–13 July 2007, Perugia, Italy (in press)

Pail R, Schuh WD, Wermuth M (2005) GOCE gravity field processing. In: Jekeli C, Bastos L, Fernandes J (eds) International association of geodesy symposia, "gravity, geoid and space missions", vol 129. Springer, Berlin, pp 36–41

Papoulis A (1984) Signal analysis. McGraw Hill, New York

Reguzzoni M (2003) From the time-wise to space-wise GOCE observables. Adv Geosci 1:137–142

Reguzzoni M, Tselfes N, Venuti G (2006) Stepwise solutions to random field prediction problems. In: Proceedings of the 6th Hotine–Marussi symposium on mathematical geodesy, Wuhan, China, 29 May – 2 June, 2006 (in press)

Rummel R, Gruber T, Koop R (2004) High level processing facility for GOCE: products and processing strategy. In: Proceedings of the 2nd international GOCE user workshop, 8–10 March 2004, Frascati, Italy, (ESA SP-569, June 2004). ISBN 92-9092-880-8, ISSN 1609-042X

Sansò F, Sideris MG (1997) On the similarities and differences between system theory and least-squares collocation in physical geodesy. Boll Geod Sci Affin, Anno LVI 2:173–206

Schuh WD (1996) Tailored numerical solution strategies for the global determination of the Earth's gravity field, Folge 81, Mitteilungen der geodätischen Institut der Technischen Universität Graz

Sideris MG (1996) On the use of heterogeneous noisy data in spectral gravity field modeling methods. J Geod 70:470–479. doi:10.1007/BF00863619

Sneeuw N, van Gelderen M (1997) The polar gap. In: Sansò F, Rummel R (eds) Geodetic boundary value problems in view of the one centimeter geoid. Lecture Notes in Earth Sciences, vol 65, Springer, Heidelberg, pp 559–568

Tscherning CC (1976a) Computation of the second–order derivatives of the normal potential based on the representation by a Legendre series. Manuscripta Geodaetica 1:71–92

Tscherning CC (1976b) On the chain-rule method for computing potential derivatives. Manuscripta Geodaetica 1:125–141

Tscherning CC (1993) Computation of covariances of derivatives of the anomalous gravity potential in a rotated reference frame. Manuscripta Geodaetica 18(3):115–123

Tscherning CC (2001) Computation of spherical harmonic coefficients and their error estimates using least squares collocation. J Geod 75:12–18. doi:10.1007/s001900000150

Tscherning CC, Rapp RH (1974) Closed covariance expressions for gravity anomalies, geoid undulations, and deflections of the vertical implied by anomaly degree–variance models. Report No. 208, Department of Geodetic Science, Ohio State University, Columbus

Visser PNAM, Sneeuw N, Gerlach C (2003) Energy integral method for gravity field determination from satellite orbit coordinates. J Geod 77:207–216. doi:10.1007/s00190-003-0315-8

Visser PNAM, van den IJssel J, van Helleputte T, Bock H, Jaeggi A, Beutler G, Hugentobler U, Svehla D (2007) Rapid and precise science orbit determination for the GOCE satellite. In: Proceedings of the 3rd international GOCE user workshop, 6–8 November 2006, Frascati, Italy (ESA SP-627, January 2007), pp 235–239. ISBN 92-9092-938-3, ISSN 1609-042X